Improving Neural Network's Robustness on Tabular Data with D-Layers

Haiyang Xia[1†], Nayyar Zaidi[2*†], Yishuo Zhang[2] and Gang Li[2]

[1]Research School of Management, Australian National University, Canberra, 2601, ACT, Australia.
[2*]Centre for Cyber Resilience and Trust (CREST), Deakin University, Geelong, 3216, VIC, Australia.

*Corresponding author(s). E-mail(s): nayyar.zaidi@deakin.edu.au;
Contributing authors: haiyang.xia@anu.edu.au;
chris.zhang@deakin.edu.au; gang.li@deakin.edu.au;
†These authors contributed equally to this work.

Abstract

Artificial Neural Networks (`ANN`) are widely used machine learning models. Their widespread use has attracted a lot of interest in their robustness. Many studies show that `ANN`'s performance can be highly vulnerable to input manipulation such as adversarial attacks and covariate drift. Therefore, various techniques that focus on improving `ANN`'s robustness have been proposed in the last few years. However, most of these works have mostly focused on image data. In this paper, we investigate the role of discretization in improving `ANN`'s robustness on tabular datasets. Two custom `ANN` layers – `D1-Layer` and `D2-Layer` (collectively called `D-Layers`) are proposed. The two layers integrate discretization during the *training phase* to improve `ANN`'s ability to defend against adversarial attacks. Additionally, `D2-Layer` integrates dynamic discretization during *testing phase* as well, to provide a unified strategy to handle adversarial attacks and covariate drift. The experimental results on 24 publicly available datasets show that our proposed `D-Layers` add much-needed robustness to `ANN` for tabular datasets.

Keywords: Robustness, Covariate Drift, Adversarial Attack, Tabular Data, Discretization

1 Introduction

The widespread use of ANN models has attracted a lot of interest in their robustness [1, 2]. Typically, one measure of ANN's robustness is to see whether it can maintain performance with the changes in input data. These changes can be driven by either malicious or benign intent. An example of malicious intent change is adversarial attacks that manipulate input data to sway the model output towards a desirable outcome [3]. An example of benign intent change is data variation over time due to covariate drift. With the ever-changing facet of adversarial attack methods and datasets drifting over time, how to add robustness to ANN on tabular datasets remains an open, yet fundamental question. This work is motivated to address the issue of robustness in ANN models by proposing new novel layers in standard ANN architecture.

Traditionally, adversarial attacks constitute imperceptible perturbations on the input image to control ANN's output. Many studies have demonstrated that the perturbed images that fail one model can also fail other models trained on different datasets with different architectures [1], highlighting the severity of the problem. In the past few years, plenty of research efforts have been exerted in designing appropriate defence mechanisms for ANN models on image datasets [2, 4]. However, image datasets are not the only datasets susceptible to adversarial attacks. Tabular datasets that are commonly used in various ANN applications domains such as finance and medicine are as vulnerable to adversarial attacks as image datasets [5]. Tabular datasets have one trait, i.e., the presence of categorical features that can serve as a natural defence against adversarial attacks, as the adversarial perturbations on categorical features can be easily observed. For instance, in a loan approval scenario, the level-of-education is bachelor, master, and doctorate – (normally represented as integers like 1, 2, and 3), it is easy for bank managers to find the fraudulent modification when a customer modifies her education level from 2 to 2.5 or from 3 to 4, to obtain a loan. However, numeric features in tabular datasets are as vulnerable to adversarial attacks as pixel values in images [5]. Considering the natural defence capability of categorical features, recently, various discretization-based defence methods have been proposed [6].

Covariate drift which informally refers to the situation where testing distribution is different from training distribution can also adversely affect ANN models' performance [7]. Several studies in domain adaptation and causal inference aim to tackle the covariate drift issue by taking advantage of the information on testing distribution [8]. Discretization can serve as a natural defence against some forms of covariate drifts as well. For example, if the Salary feature (at the training time) is discretized with equal frequency discretization into three bins {A, B, C} – even with covariate drift resulting in the monotonic transformation of the testing data – discretization on the transformed Salary feature (at the testing time) can result in a similar allocation of the bins.

Given the pivotal role that discretization can play as a defence mechanism against adversarial attacks and covariate drift, there is a need to integrate

discretization into ANN's models for increasing their robustness. In this work, we propose two customized new layers for ANN – named D1-Layer ('**D**iscretization') and D2-Layer ('**D**ynamic **D**iscretization') – collectively called D-Layers, to address this need. The main motivations of these two layers are:

- Existing discretization-based adversarial attack defence methods [6, 9] normally discretize data prior to training the model. Despite their effectiveness, if some part of the training data is changed (e.g., as part of adversarial training), the discretization results will be incorrect, as the discretization boundaries are learned beforehand. Furthermore, any time the model is to be re-trained requires re-discretizing the dataset. The seamless integration of discretization in ANN (during model training) and exploiting its benefits is the main motivation for our proposed D-Layers.
- Once the model is trained, there is no way to update the discretization boundaries. However, if the distribution of testing data is changed due to covariate drift or adversarial attack, there is a strong need to update discretization boundaries to accommodate this distribution change. In other words, we need dynamic discretization at the testing phase to resist potential distribution changes caused by covariate drift or adversarial attack. The seamless integration of such dynamic discretization in ANN (during model testing) is the main motivation for our proposed D2-Layer.

The main contributions of this paper are:

- We have proposed two new layers for adding robustness to ANN models. Specifically, D1-Layer integrates discretization during the training phase to improve ANN's ability to defend against adversarial attacks. Whereas, D2-Layer integrates discretization during the training phase, as well as during the testing phase to provide a unified strategy for ANN to handle covariate drift and adversarial attacks.
- We demonstrate that our proposed D1-Layer lead to the state-of-the-art (SOTA) defence mechanism against a range of standard attacks on various publicly available tabular datasets.
- We demonstrate that our proposed D2-Layer offers an effective unified strategy to address adversarial attacks and covariate drift at the same time.

The rest of this paper is organized as follows. In Section 2, we review the related works. In Section 3, we present our proposed formulations namely D-Layers. Section 4 provides an empirical evaluation of our proposed formulations. In Section 5, we conclude the paper with pointers to future works.

2 Related work

2.1 Adversarial Attack Methods

To highlight the robustness of ANN models, a large number of adversarial attack models have been proposed in the literature in the past few years. Broadly, these existing adversarial attack models can be divided into white-box attack

models and black-box attack models [10]. Attack models that require access to information of the original ANN model such as parameters, gradient, or structure to conduct attacks are referred to as white-box attack models, otherwise black-box attack models [11]. Our study focuses on white-box attack models and hence we will mainly review popular white-box attack models. A more comprehensive literature review can be found in [11, 12].

FGSM (Fast Gradient Sign Method) [1] is the most classic white-box attack model for both image and tabular data. It creates adversarial samples by adding gradients to the original instance. FGSM is easy to implement but normally has a relatively low success rate, as the adversarial samples created by adding gradient may be insufficient to cross the decision boundary [4]. A direct extension of FGSM is BIM (Basic Iterative Method) which iteratively conduct FGSM multiple times with a small step size to achieve better attack performance [13]. PGD (Projected Gradient Descent) is also a popular white-box attack model built on top of FGSM [14]. Different from BIM that directly iteratively conducts FGSM from the original sample, PGD initializes the start of the adversarial attack from a random distribution to add variations to the attack to further improve the attack's success rate.

Another popular white-box attack model is DeepFool [15]. It works by iteratively linearizing the model to generate unperceivable adversarial examples. Compared with other gradient-based white-box attack models, DeepFool is more efficient as it can always generate adversarial examples that are close to the decision boundary. LowProFool is the state-of-the-art white-box attack model on tabular data [16]. It induces parameter updates toward the targeted class by utilizing the gradient of adversarial noise. The importance weights of features are evaluated to ensure large perturbations only exist on irrelevant or less important features, such that the generated examples are imperceptible to expert scrutiny.

2.2 Adversarial Defence Methods

Madry [14] is the most straightforward defence method – it takes advantage of adversarial training to minimize models' adversarial risk to defend against adversarial attacks. Despite its effectiveness, one critical issue of this adversarial-training-based defence model is overfitting to attacks that generate adversarial samples [2]. E.g., the models that were adversarially trained to resist FGSM frequently failed to resist L-BFGS and BIM attacks. Thereby, recent studies have started to advocate input discretization as the defence mechanism. Thermometer encoding [6] is one of the most popular discretization-based defence models as it defends against adversarial attacks by discretizing the numeric inputs to $[0, 1]$ vectors. For example, discretizes 0.23 to $[0, 0, 1, 1, 1, 1, 1, 1, 1, 1]$, 0.34 to $[0, 0, 0, 1, 1, 1, 1, 1, 1, 1]$, etc. Thermometer's formulation is very similar to one-hot encoding, but it can preserve the order of input after discretization, thus having better performance than one-hot encoding. In the context of deep ANN models implemented via Keras [1], one

[1] https://keras.io/

can utilize Keras discretization layer [2]. It offers another method to discretize neural network input. It is important to note that unlike other discretization methods which are feature-based (i.e., different cut-points are learned for different features) – the discretization strategy in this layer learns one set of cut-points for all the features – i.e., data across all features is used to compute the quantiles – which are later used as the cut-points to discretize. Little efforts have been made to investigate the effectiveness of `keras` discretization layer in defending against adversarial attacks. We will explore this direction together by proposing two discretization-inspired algorithms in this work.

`D2A3` and `D2A3N` [9] are state-of-the-art defence models on tabular data. `D2A3` defends against adversarial attacks by exploiting both input discretization and adversarial training. In `D2A3`, the numeric input features are discretized to train a discretized model – this model is then improved by taking advantage of adversarial training. The main limitation of `D2A3` is the requirement for accessing input data and changing it from numeric to discrete, which may be impossible in many application scenarios. In `D2A3N`, the numerical input features are discretized by the cut-points directly learned from the training data – data close to cut-points are considered adversarial samples and are replaced by the median of the bin to defend against adversarial attacks. Although these existing studies demonstrated the effectiveness of input discretization as a defence mechanism against tabular data adversarial attacks, their performance can be further improved by integrating flexible within model cut-points learning strategies as well as dynamic discretization – strategies that we will study in this work. Note, `D2A3` and `D2A3N` are state-of-the-art adversarial defence approaches in the context of deep `ANN`. Therefore, we will consider these approaches as the baseline when comparing the adversarial defence capability of the proposed methods in this work. The main advantage of our proposed `D-Layers` over `D2A3` and its variant is that the defence mechanism does not include adversarial training. Secondly, and importantly, our proposed method integrates discretization in the learning of an `ANN` model, unlike a pre-discretization strategy of `D2A3`. We will discuss in the following, that this trait is one of the reasons for the superior performance of `D-Layers`. One limitation of our proposed approach in handling covariate drift is its inability to handle non-monotonic transformations (or drifts). This is because, as we will also discuss below, `D-Layers` are based on equal frequency discretization, and hence assumes that order is preserved during the drift. However, if the order is not preserved, our proposed layers will not be effective. We are working on how to handle non-monotonic drifts as well as concept drift as an extension of this research.

2.3 Covariate Drift

Covariate drift also known as covariate shift represents a typical model drift scenario that occurs when the distribution of the testing data is different from the training data [17]. In covariate drift, the distribution change only lies in the

[2] https://keras.io/api/layers/preprocessing_layers/categorical/discretization/

input features, whilst the labels of testing data remain the same [18]. The case in which the labels of the testing data change as well is called *concept drift* [19] – which is outside the scope of this work. Covariate drift can significantly compromise the performance of a well-trained ANN, therefore, a bunch of studies on domain adaptation [20] and transfer learning [21] have been conducted to address the covariate drift problem through the alignment of training and testing distributions [22]. E.g., [23] proposed a kernel mean matching-based method to match the training and testing distributions by reweighting the training distribution in a reproducing kernel Hilbert space. [24] proposed an important weighting method for addressing the covariate drift by reweighting the residuals of kernel mean matching and non-parametric regression. [25] proposed a strategy that learns the weights required to address covariate shifts in only one step. [26] proposed a new measurement to measure the distribution mismatch between training and testing data based on the integrated ratio of probabilities of balls at a given radius, and demonstrated its effectiveness in addressing covariate drift in non-parametric regression. The main limitation of these approaches is the dependence on the prior knowledge of testing data that is not always available at the training stage [27]. Although some recent studies on causal inference have tackled this issue by utilizing the stability of causal graphs [28], the proposed models are complicated due to the difficulty of capturing causal relations in the data. This paper will show that simple input discretization can be an effective method to handle some forms of covariate drift, i.e., monotonic covariate drift.

Covariate and concept drift have been widely studied in machine learning, however, most of this work aims to develop models that have a built-in mechanism to handle either concept or covariate drift, e.g., [29–31]. Our work, in this paper, is different from various existing works, as we specifically are interested to address covariate drift in deep ANN models. Therefore, we have not conducted a comparison with the existing concept or covariate drift method in this work, as it does not offer a meaningful comparison. We, however, are interested to do this analysis as part of future works for this research. Note, the baseline for measuring the effectiveness of our proposed method in handling covariate drift is a vanilla deep ANN model.

3 Methodology

In this section, we start by formulating the problem of robust ANN, followed by discussing the motivations for using discretization to improve ANN's robustness. Later, we present in detail our proposed D1-Layer and D2-Layer.

3.1 Problem formulation

Definition 1 (Adversarial Attack on Tabular Data.) Let $(\mathbb{X}, \mathbb{Y}) = \{(X^1, Y^1), (X^2, Y^2), \ldots, (X^n, Y^n)\}$ be a dataset with n samples, where $\mathbb{X}$ is defined by a set of features $j \in \mathbb{J}$, $\mathbb{Y} = [Y^1, Y^2, \ldots, Y^n]$ denotes the corresponding labels. Let $f : \mathbb{R}^D \rightarrow \mathbb{Y}$ be the trained ANN model. For a given sample $(X^i, Y^i) \in (\mathbb{X}, \mathbb{Y})$, the

adversarial attack aims to generate an adversarial sample $X^i_{\text{adv}} = (X^i + r^*)$ such that

$$\begin{aligned} f(X^i_{\text{adv}}) = Y^t \neq f(X^i) = Y^i \\ \text{s.t. } X^i_{\text{adv}} \in \mathbb{R}^D \text{ and } r^* = \arg\min_r d(r), \end{aligned} \tag{1}$$

where Y^t is the target label, $d(r) = \|r\|_p$ is the perceptibility value that indicates the quantity of the changes in X^i after adding adversarial perturbation r. r^* is perturbation r that achieves minimum $d(r)$.

Definition 2 (Covariate Drift.) For a model $f : \mathbb{X} \to \mathbb{Y}$ covariate drift refers to the case where $P_{\text{train}}(Y \mid X) = P_{\text{test}}(Y \mid X)$, while $P_{\text{train}}(X) \neq P_{\text{test}}(X)$.

Here, $P_{\text{train}}(X)$ is the distribution of the training data (without labels), $P_{\text{test}}(X)$ is the distribution of the testing data (without labels), $P_{\text{train}}(Y \mid X)$ is the conditional distribution of training data, and $P_{\text{test}}(Y \mid X)$ is the conditional distribution of testing data.

Given definition 1 and definition 2, we have the following definition for robust `ANN`:

Definition 3 (Robust `ANN`.) For a model $f : \mathbb{X} \to \mathbb{Y}$ trained on the training dataset $\mathcal{S}_{\text{data-train}} = (\mathbb{X}, \mathbb{Y})$, suppose its performance on the testing dataset $\mathcal{S}_{\text{data-test}}$ is $D\%$. For a perturbed dataset $\tilde{\mathcal{S}}_{\text{data-test}}$ (based on definitions 1 and 2), f is robust if its performance on $\tilde{\mathcal{S}}_{\text{data-test}}$ is not less than $D\% - \delta$, where δ is a user-specified confidence interval.

We will make use of this definition to evaluate (and compare) the effectiveness of our proposed formulations.

3.2 Rationales

Discretization is performed by sorting the data and separating the numeric features into different bins according to the learned cut-points (also known as discretization boundaries) [3]. Figure 1 demonstrates the rationale of discretization-based adversarial attack defence methods. As shown in Figure 1a, in the original numeric feature space, there is no way to differentiate adversarial example x_{adv} and other data. However, after discretization, the numeric features will be separated into different bins according to specific cut-points (see Figure 1b). The bin number (e.g., 1, 2, 3, 4) or the median/mean of bin values will be used to train the `ANN` models. It can be seen that after discretization the adversarial example x_{adv} has been scaled back to a value that is expected by `ANN` (in our example, they are $1, 2, 3, 4$). That means, whatever the attacker's intent was, discretization is able to convert adversarial samples back to the values that have a consistent format with training samples. The

[3]The cut-points are obtained based on different strategies, such as `MDL`, `Equal Frequency` (`EF`), etc.

efficacy of this approach depends on the number of discretized values that cross the bin boundaries. For example, if x_{adv} in Figure 1b moves to the right of δ_3 – its discretized value will be incorrect (see Figure 2a), thereby leading to performance degradation. Furthermore, as shown in Figure 2b, a small drift of the data on the x-axis (covariate drift) will result in many data points being assigned to the wrong bins or even invalid bins. Based on this analysis, the following observations can be drawn:

1. Pre-discretizing the data is not an effective defence strategy [4], as the pre-learned cut-points are learned on original data, and are static. Every time data is modified, we must re-compute the cut-points and re-train the model (which can be expensive), to make discretization work as a defence strategy. Note, we are assuming that we have access to some adversarial or drifted data at the training time. There is a need for cut-points to be adjusted based on updated data during the training – we will call this *dynamic discretization*. Our proposed `D-Layers` are aimed at incorporating dynamic discretization for adding robustness to the `ANN` model.
2. Cut-points should be dynamically updated from the data even during the testing time. If the data distribution is changed during the testing time (i.e., covariate drift), the cut-points should be changed accordingly to accommodate the changes to maintain discretization accuracy. Similar to batch normalization [32], our proposed `D2-Layer` aims to address this issue by taking advantage of the statistical information of testing data.

3.3 D1-Layer

Let us start by formulating our problem. Ideally, we are interested in discretizing an input feature's numeric value, in an `ANN` model, i.e., a value say

[4] Note, `D2A3N` adopts the strategy of pre-discretization

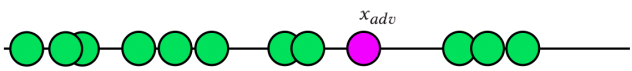

(a) Adversarial data in numeric feature space.

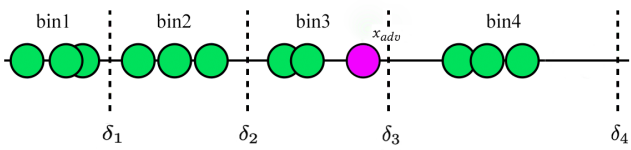

(b) Adversarial data in discretized space.

Fig. 1: Rationale of discretization-based defence models.

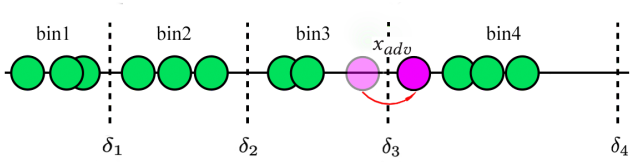

(a) Data change caused by Adversarial Attacks.

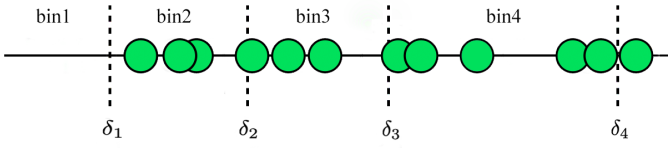

(b) Data change caused by covariate drift.

Fig. 2: Illustration of limitations of stationary cut-points in case of adversarial attack and covariate drift.

23.5 is transformed into value say 3, based on some cut-points – $\delta_1, \ldots, \delta_k$. Our problem constitutes learning the cut-points in an end-to-end fashion, such that the whole process remains differentiable. For this, we have proposed a novel layer named `D1-Layer`, that does exactly that. The idea of `D1-Layer` is inspired by `VQ-VAE` (Vector Quantized Variational Auto-Encoder) that discretizes the encoder's output via a codebook to improve the quality of image generation [33]. In `D1-Layer`, we aim to learn a cut-point space. We denote this space as – $\mathcal{C}$, also known as the codebook. This codebook will be used to discretize the input features. E.g., the simplest way to discretize a data point is by doing a nearest neighbour search in the codebook, i.e., the input data is represented by the index of the nearest codebook vector.

The salient feature of `D1-Layer` is that it actually aims to learn the codebook space which is basically the representation of the cut-points, i.e., the cut-point δ_i is actually represented by a D-dimensional vector. The number of cut-points has to be specified in advance, e.g., if we have K cut-points, we have $\mathcal{C} \in \mathbb{R}^{K \times D}$. An issue that originates from enforcing the dimensions of the cut-point to be $1 \times D$, is the dimensionality mismatch between an input data feature (a scale) and the cut-point representation (a vector of size D). This renders the comparison between input data feature and codebook vector (or nearest neighbour search) invalid. `D1-Layer` utilizes three strategies to address this dimensionality mismatch [5]. Let us discuss these strategies in the following.

[5] All three forms of representation assume that the input features are normalized by a min-max scaling.

3.3.1 Duplicate Expansion Search (DES)

The first strategy that D1-Layer employs is to duplicate the scalar value D-times to convert it into a D-dimensional vector. This is depicted in Figure 3a. Let $\mathcal{Z}(\cdot)$ indicate an operator that takes a scalar value as input and returns a vector of size D. Formally, for the j-th feature of the data i, the duplicate expansion search can be defined as:

$$\mathcal{Z}(X_j^i) = \underbrace{[X_j^i, X_j^i, \ldots, X_j^i]}_{D}.$$

3.3.2 Taylor Series Expansion Search (TSES)

Considering simple duplication may have less variation on the input representations, D1-Layer also employs a Taylor series expansion of $\frac{1}{1-X_j^i}$ to expand the scalar value (as shown in Figure 3b). Formally, the Taylor series expansion search can be defined as:

$$\mathcal{Z}(X_j^i) = [X_j^i, (X_j^i + {X_j^i}^2), \ldots (X_j^i + {X_j^i}^2 + \ldots + {X_j^i}^D)].$$

For simplicity, we ignored the constant 1 in the Taylor series expansion.

For DES and TSES, after aligning the dimensionality of input features and codebook, the nearest neighbor search can be defined as:

$$q(X_j^i) = \text{argmin}_k \, \|\mathcal{Z}(X_j^i) - \mathcal{C}_k\|_2. \tag{2}$$

3.3.3 Direct Cut-point Search (DCS)

Other than expanding our input values to match the size of the cut-point space, one can also reduce the dimensionality of the cut-point space to match the input size. As shown in Figure 3c, in DCS, we set the dimensionality of the cut-point space to $1 \times K$. The discretized value $q(X_j^i)$ can then be determined as:

$$q(X_j^i) = \text{argmin}_k \, \|X_j^i - \mathcal{C}_k\|_2. \tag{3}$$

3.3.4 Learning in D1-Layer

The output of D1-Layer is the discretized data – $q(X_j^i)$, that is passed through to the next layer for further processing. The forward pass through D1-Layer can be seen as the clustering of the input feature values – the index of each cluster center served as the discretized value.

The main challenge in training D1-Layer is that Equations 2 (or 3) is non-differentiable due to the presence of the argmin operation. Similar to VQ-VAE, the simple gradient estimator strategy is adopted to address this issue [34]. That is, in the backward pass, gradients of the numeric representations are approximated by directly copying the gradient of the discretized representations (see Figure 3). The loss function of our proposed D1-Layer-based ANN

is:

$$L = L_c(Y^i, X^i) + \sum_{j=1}^{|\mathbb{J}|} \|\mathbf{sg}[Z(X_j^i)] - \mathcal{C}_k\|_2^2, \tag{4}$$

where $L_c(Y^i, X^i)$ represents the standard classification loss such as cross-entropy, `MSE`, etc. $|\ \mathbb{J}\ |$ represents the number of features, $\sum_{j=1}^{|\mathbb{J}|} \|\mathbf{sg}[q(X_j^i)] - \mathcal{C}_k\|_2^2$ represents the codebook learning loss of data X^i, which directs the codebook embedding $\mathcal{C}_k$ toward the corresponding data value. Note, $\mathbf{sg}[\cdot]$ is the stop gradient operator that has zero partial derivatives.

We have summarized the learning process of `D1-Layer`-based `ANN` in Algorithm 1. In the training phase, `D1-Layer` first discretizes the input data of each mini-batch – we denote discretized data as $q(X)_b$ (Algorithm 1, lines 1-12). Note, we provide algorithm for `TSES` representation. Discretized data $q(X)_b$ is then used in subsequent layers to train the network with parameters Θ and codebook $\mathcal{C}$ (Algorithm 1, lines 13-20). In the testing phase, the learned codebook $\mathcal{C}$ is used to discretize the input data, which is then fed into the network parameterized by parameter Θ, for inference (Algorithm 1, lines 21-30).

3.4 D2-Layer

`D1-Layer` utilizes an objective function of the form of Equation 4 to learn a representation of the cut-points. A simpler strategy could be to use the statistical information present in each mini-batch of the data and adjust cut-points accordingly. Our proposed `D2-Layer` does exactly that. It takes advantage of the statistical information of each mini-batch to dynamically update the cut-points (which can be applied at training as well as testing time).

Let $\mathcal{B} = [\mathbb{X}_1, \cdots, \mathbb{X}_B]$ represent a mini-batch of size B. `D2-Layer` sorts the data in each mini-batch and calculates the cut-points using `Equal Frequency` (`EF`) discretization. Other forms of discretization can be used, however, we argue that `EF` discretization has desirable properties that can lead to some robustness in the model.

Let $\Phi_{\texttt{EF}}(\mathbb{X})$ represent a discretization function that returns a set of K cut-points (based on `EF` discretization), learned on mini-batch $\mathbb{X}$:

$$\Phi_{\texttt{EF}}(\mathbb{X}) \sim [\delta_1, \cdots, \delta_K]. \tag{5}$$

We have discretized value $q(X_j^i) = \mathbb{O}(\hat{\Phi}(X_j^i))$. Here, $\hat{\Phi}(.)$ is the function that applies the learned cut-points $\Phi_{\texttt{EF}}(\mathbb{X})$ to the data, and $\mathbb{O}(.)$ is the function that represents the discretized value, e.g., one-hot-encoding, bin-number, etc. The discretized value $q(X_j^i)$ is then used in subsequent layers of `ANN` to train the network. Let us discuss some salient features of `D2-Layer`:

1. The mean and variance of the output of the `D2-Layer` are guaranteed to be stationary and, therefore, the covariate drift can be largely eliminated (in cases where drift is due to monotonic transformation).

Algorithm 1 D1-Layer embedded `ANN`

Input: $\mathcal{S}_{\text{data}} = (\mathbb{X}, \mathbb{Y})$, length-of-embedding-vector D, number-of-embeddings K, search-strategy $\in \{\texttt{DES}, \texttt{TSES}, \texttt{DCS}\}$ (default is `TSES`)

`/* ` $\mathcal{S}_{\text{data}}$ `is split into` $\mathcal{S}_{\text{train}}$ `and` $\mathcal{S}_{\text{test}}$ `*/`
`/* Training starts */`
Initial parameters: $\boldsymbol{\theta}$ and $\mathcal{C}$, of the model $f : \mathbb{X} \rightarrow \mathbb{Y}$
for iteration $t \subset T$ in training **do**
  for b-th mini-batch $(\mathbb{X}, \mathbb{Y}) \in \mathcal{S}_{\text{train}}$ **do**
    for i-th data in the batch $(\mathbb{X}_b)$ **do**
      `/* Taylor Series Expansion */`
      for j-th feature in the data **do**
        $\mathcal{Z}(X_j^i) = [X_j^i, (X_j^i + {X_j^i}^2), \ldots (X_j^i + {X_j^i}^2 + \ldots + {X_j^i}^D)]$
        $q(X_j^i) = \text{argmin}_k \|\mathcal{Z}(X_j^i) - \mathcal{C}_k\|_2$ `// Equation 2`
      end
    end
    `/* Denoting` $q(X)_b$`, the output of discretized batch` b `*/`
    Forward propagate $q(X)_b$ through hidden layers
    Calculate gradients w.r.t $\boldsymbol{\theta}$ and $\mathcal{C}$ – denoted as $\nabla_{\boldsymbol{\theta}}$ and $\nabla_{\mathcal{C}}$
    `/* Update parameters with default Adam optimization */`
    $\boldsymbol{\theta}^{t+1} \leftarrow \boldsymbol{\theta}_s^t + \eta \nabla_{\boldsymbol{\theta}}$, $\mathcal{C}^{t+1} \leftarrow \mathcal{C}_s^t + \eta \nabla_{\mathcal{C}}$
  end
end
return f parameterized by $\boldsymbol{\theta}$ and $\mathcal{C}$
`/* Testing starts */`
for i-th data in $(\mathbb{X}, \mathbb{Y}) \in \mathcal{S}_{\text{test}}$ **do**
  `/* Taylor Series Expansion */`
  for j-th feature in the data **do**
    $\mathcal{Z}(X_j^i) = [X_j^i, (X_j^i + {X_j^i}^2), \ldots (X_j^i + {X_j^i}^2 + \ldots + {X_j^i}^D)]$
    $q(X_j^i) = \text{argmin}_k \|\mathcal{Z}(X_j^i) - \mathcal{C}_k\|_2$ `// Equation 2`
  end
  Forward propagate $q(X^i)$ through hidden layers
  return $f(q(X^i))$
end

2. The discretization operator used in `D2-Layer` is not differentiable, hence, the gradient-based attacking for original input X^i will not be effective. Thus providing a defence against many forms of adversarial attacks.
3. `D2-Layer` can be deployed at the testing time – i.e., the cut-points can be adjusted based on testing data distribution – making it perfect to address covariate drift even after the model is trained. Note, one can re-train a codebook in `D1-Layer` at testing time, but this might not be effective, as learning a codebook representation of size $K \times D$ requires much larger data and hence larger size of the batch. On the contrary, `D2-Layer` makes use

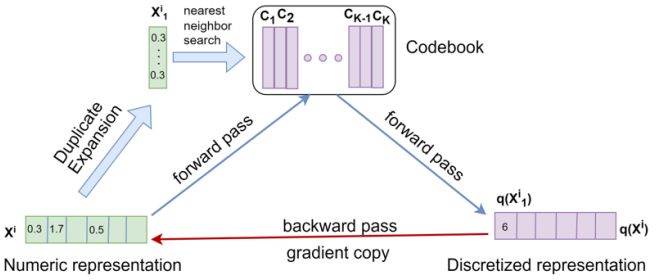

(a) Duplicate expansion search (`DES`).

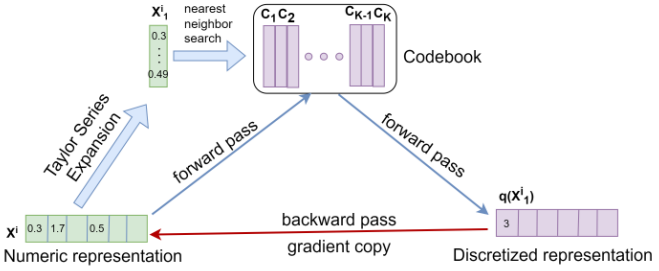

(b) Taylor series expansion search (`TSES`).

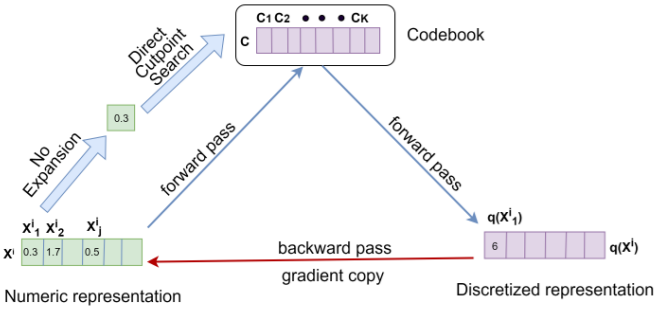

(c) Direct cut-points search (`DCS`).

Fig. 3: Illustration of the discretization in `D1-Layer`. The numeric input in each feature is discretized by the codebook. The gradient of discretized feature representation will be directly copied to the numeric feature representation in the backward pass (straight-through estimator).

of simpler statistics from the data, which can be obtained from a few test data points.

We have summarized the learning of the `D2-Layer`-based `ANN` at Algorithm 2.

Algorithm 2 D2-Layer embedded `ANN`

Input: $\mathcal{S}_{\text{data}} = (\mathbb{X}, \mathbb{Y})$, bin number m

1 /* $\mathcal{S}_{\text{data}}$ is split into $\mathcal{S}_{\text{train}}$ and $\mathcal{S}_{\text{test}}$ */
2 /* Training starts */
3 Initial parameters: $\boldsymbol{\theta}$, of the model $f : \mathbb{X} \rightarrow \mathbb{Y}$
4 **for** iteration $t \subset T$ in training **do**
5 **for** b-th mini-batch $(\mathbb{X}, \mathbb{Y}) \in \mathcal{S}_{\text{train}}$ **do**
6 /* Learn EF cutpoints on batch b */
7 $\Phi_{\text{EF}}(\mathbb{X}_b) \sim [\delta_1, \cdots, \delta_K]$
8 **for** i-th data in the batch $(\mathbb{X}_b)$ **do**
9 **for** j-th feature in the data **do**
10 $q(X_j^i) = \mathbb{O}(\hat{\Phi}(X_j^i))$ // Discretization
11 **end**
12 **end**
13 /* Denoting $q(X)_b$, the output of discretized batch b */
14 Forward propagate $q(X)_b$ through hidden layers
15 Calculate gradients w.r.t $\boldsymbol{\theta}$ – denoted as $\nabla_{\boldsymbol{\theta}}$
16 /* Update parameters with default Adam optimization */
17 $\boldsymbol{\theta}^{t+1} \leftarrow \boldsymbol{\theta}_s^t + \eta \nabla_{\boldsymbol{\theta}}$
18 **end**
19 **end**
20 **return** f parameterized by $\boldsymbol{\theta}$
21 /* Testing starts */
22 **for** b-th mini-batch $(\mathbb{X}, \mathbb{Y}) \in \mathcal{S}_{\text{test}}$ **do**
23 /* Re-Learn EF cutpoints on batch b */
24 $\Phi_{\text{EF}}(\mathbb{X}_b) \sim [\delta_1, \cdots, \delta_K]$
25 **for** i-th data in the batch $(\mathbb{X}_b)$ **do**
26 **for** j-th feature in the data **do**
27 $q(X_j^i) = \mathbb{O}(\hat{\Phi}(X_j^i))$ // Discretization
28 **end**
29 **end**
30 Forward propagate $q(X^i)$ through hidden layers
31 **return** $f(q(X^i))$
32 **end**

In the training phase of `D2-Layer`, equal frequency discretization is used to learn the cut-points of each training batch (Algorithm 2, lines 1-12). The discretized values resulting from the learned cut-points are used to train the entire network (Algorithm 2, lines 13-20). The selection of feature-specific equal-frequency discretization is critical to the working of `D2-Layer`'s algorithm – i.e., in handling covariate drift, and in warding-off adversarial attack. As we mentioned earlier, `Keras` discretization layer also learns cut-points but based

Table 1: Statistic Information of Datasets

Dataset	n	m_n	m_c	Dataset	n	m_n	m_c
covtype	581012	10	44	sign	12546	9	3
census-income	299285	35	5	occupancy	10129	14	2
skin-segmentation	245057	4	2	satellite	6435	37	6
localization	164860	2	3	page-blocks	5473	11	5
accelerometer	153001	4	0	wall-following	5456	25	4
higgs	98050	28	0	waveform-5000	5000	21	0
ipums.la.99	88443	23	38	spambase	4601	58	2
connect-4	67557	43	3	kr-vs-kp	3196	0	36
adult	48842	6	8	sick	3772	6	21
letter-recog	20000	17	26	hypothyroid	3163	6	19
magic	19020	11	2	cmc	1473	2	7
gassensor	13790	128	0	german	1000	3	17

on the quantiles of the whole input data rather than separately for each feature. We will integrate this quantiles-based discretization strategy in `D2-Layer` and compare it with other forms of discretizations later in Section 4.

In the testing phase, different from `D1-Layer` and other existing defence methods that use cut-points learned from training data, `D2-Layer` uses equal frequency discretization to learn new cut-points from each testing batch to ensure the cut-points are suitable for testing data (Algorithm 2, lines 21-32). This dynamic discretization strategy makes sure that `D2-Layer` can handle distribution drifts during the testing phase.

4 Experiments

In this section, we start by presenting the details of our experimental settings followed by the results and detailed analysis.

4.1 Experimental Settings

4.1.1 Datasets

We have used 24 classification datasets from UCI machine learning dataset repository [6]. All of these datasets have more than 1000 samples. Of the considered datasets, there are 5 datasets with more than 100,000 samples and are denoted as `Large`, 9 datasets with between 10,000-100,000 samples and are denoted as `Medium`, 10 datasets with between 1,000-10,000 samples and are denoted as `Small`. The statistics information of these datasets is shown in Table 1, where n, m_n, and m_c represent the number of samples, numeric features, and categorical features individually.

[6] https://archive.ics.uci.edu/ml/datasets

4.1.2 Baseline Methods and Evaluation Metric

In terms of adversarial attacks, three of the most commonly used white-box attack models, namely, `FGSM`, `DeepFool` (`DPF`), and `LowProFool` (`LPF`) have been adopted in our experiments. The parameters of these models are set as the values suggested in the respective original papers, e.g., the step size of `FGSM` is set to 0.1, the maximum iteration of `LowProFool` and `DeepFool` is set to 50, the trade-off factor of `LowProFool` is set to 10.

For defence, the state-of-the-art tabular data adversarial attack defence model `D2A3N` and `Madry` are selected as the baselines to test `D-Layers` embedded `ANN`'s robustness. The `ANN` model without any defence method (denoted as `Clean`) is used as the baseline to demonstrate the severity of the robustness problem. The standard evaluation metric `Robust Accuracy` is used to evaluate our proposed `D-Layers`' performance in defending against adversarial attacks. Similar to `Standard Accuracy` that measures the ratio of correct predictions and total data points, `Robust Accuracy` measures model's accuracy under unsettled conditions such as attack and covariate drift [9] – the higher the `Robust Accuracy`, the more robust the model, and vice-versa.

4.1.3 Implementations

`D-Layers` and all baselines are implemented with `PyTorch`. `D1-Layer` and `D2-Layer` are integrated into the first layer of an `ANN` that has 5 hidden layers with `ReLu` activation function and `Softmax` as the output layer. Each of the hidden layers has 100 neurons. The `training epochs`, `batch size`, and `learning rate` is set to 500, 100, and 0.0001 respectively. The number of bins K is set to 5 for both `D1-Layer` and `D2-Layer`. Embedding dimensions – D, in `D1-Layer` is set to 10. For the implementation of adversarial attack models, we use the code released in the original papers, which is available on GitHub [7]. For `D2A3N`, we implement the `Equal Frequency` discretization-based version without adversarial training for fair comparison (i.e., denoted as `D2A3N-EF` in the original paper). The parameters of `D2A3N` and referred attack models are set to the default values as provided in the paper. All the experiments were conducted on an $i7-10750$ desktop PC with 16 GB RAM and single NVIDIA GeForce GTX 1660 Ti GPU.

4.1.4 Evaluation Scenario

To evaluate the effectiveness of our proposed `D-Layers` in improving `ANN`'s robustness, we split the data into *training set* and *testing set*. The testing data is attacked via three attack methods as presented in Section 4.1.2 or modified with covariate drift. We will discuss the details of concept drift in the later section. Nonetheless, we call the data *modified testing data*. The proposed `D-Layers` formulation and other baselines are trained with *training data*. The performance of the trained model is evaluated on the *modified testing data*. The two-fold cross-validation is adopted for the train-test split, and the

[7] https://github.com/axa-rev-research/LowProFool

average robust accuracy results over five rounds are reported. The evaluation framework is illustrated in Figure 4.

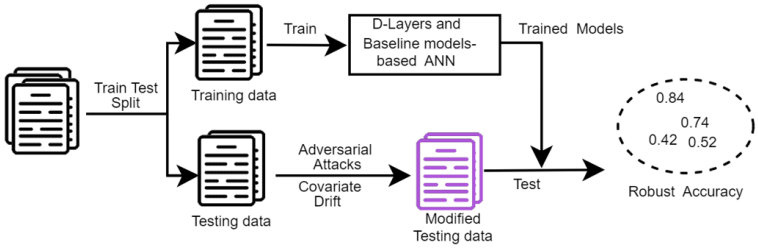

Fig. 4: The evaluation framework of the experiments.

4.2 Experimental Results

4.2.1 Comparison of `D1-Layer` Search Strategies

Before comparing the defence performance (robust accuracy) against adversarial attacks of our proposed `D-Layers` with baselines, we need to determine the best search strategy for `D1-Layer`. For this, we compared the performance of `D1-Layer` embedded `ANN` with three different search strategies, i.e., `DES`, `TSES`, and `DCS`. The average robust accuracies are presented in Figure 5 [8], where the results are broken across all, large, medium and small categories of datasets. Three attack methods of `FGSM`, `LPF` and `DPF` are used. It can be seen that in most cases `TSES` has higher robust accuracy than `DES` and `DCS` in defending all baseline attack methods (especially, in face of `LPF` attack). The pattern is consistent across `Large` and `Medium` datasets. On `Small` datasets, `DCS` performs better than other search strategies. For sake of simplicity, in the remainder of this paper, we only present `D1-Layer` results with `TSES` as representative of the three search techniques. The potential of `ANN` models is best-achieved with `Large` datasets. This is because on `Medium` and `Small` datasets, they can overfit the data. Our selection of `TSES` as representative is motivated by its extremely good performance of itself on `Large` collection of datasets.

4.2.2 Defence Against Adversarial Attacks

Let us now compare the performance of our proposed `D-Layers` with other baselines in terms of defending against adversarial attacks. The average robust accuracies of these methods are shown in Figure 6 [9].

[8] The detailed robust accuracy of `D1-Layer` under the three search strategies on each dataset is provided in Table 1 of the appendix.

[9] The detailed performance of `D-Layers` and baselines in defending against adversarial attacks on each dataset is provided in Table 2 of the appendix.

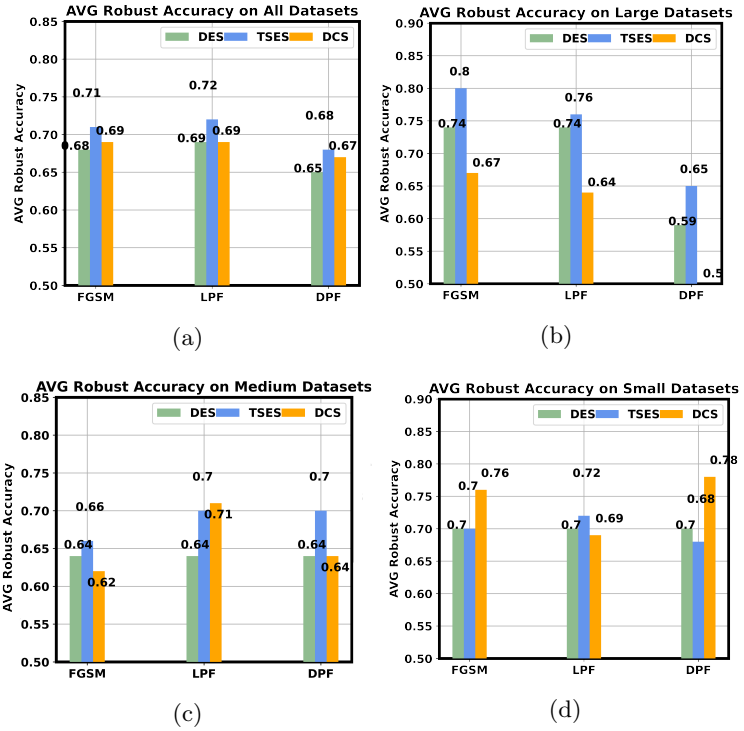

Fig. 5: Robust Accuracy comparison of different search strategies for `D1-Layer`, under adversarial attacks.

From Figure 6a, we can see that both `D1-Layer` and `D2-Layer` demonstrate higher robust accuracies than baselines on all datasets. This demonstrates the effectiveness of our proposed `D-Layers` in defending against adversarial attacks. The average robust accuracies of `Clean ANN` on all 24 datasets under `FGSM`, `LPF`, and `DPF` attacks are merely 0.37, 0.24, and 0.26 respectively. These alarming lower robust accuracies demonstrate that white-box adversarial attacks are quite effective in degrading the performance of `ANN` models. The higher average robust accuracy of `D2A3N` and `Madry` compared to `Clean ANN` demonstrates their effectiveness in defending against adversarial attacks. It is important to note that `D2A3N` is the state-of-the-art defence model. Let us compare the performance of `D-Layers` with `D2A3N` and `Clean ANN` in the following.

It is encouraging to see that `D2-Layer` leads to a performance improvement of 12%, 9%, and 14% on `FGSM`, `LPF`, and `DPF` attacks respectively over `D3A3N`. Compared with `Clean ANN`, the average robust accuracy improvement of `D2-Layer` on these three attacks reaches 34%, 48%, and 42% respectively.

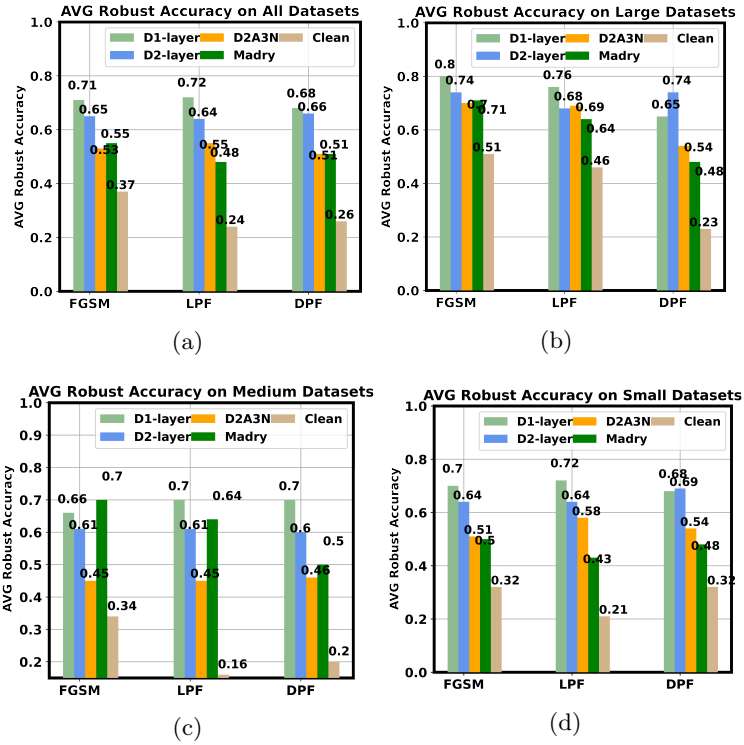

Fig. 6: Robust Accuracy of `D1-layer`, `D2-layer` and baselines under adversarial attacks.

It can be seen that `D1-Layer` achieves the highest average robust accuracy when compared with all other baselines. The average robust accuracy improvement of `D1-Layer` defence against `FGSM`, `LPF`, and `DPF` attacks compared to `D2A3N` reaches 18%, 17%, and 17% respectively; and that robust accuracy improvement compared to `Clean ANN` reaches 34%, 48%, and 42% respectively.

From Figure 6b Figure 6c, and Figure 6d, we can see that `D1-Layer` wins against all baselines on almost all categories of datasets, the exception is `Large` with `DPF` attack. `D2-Layer` also shows superior performance on almost all categories of datasets, exceptions are `Medium` with `FGSM` and `LPF` attacks. Generally, we can conclude that in most cases `D1-Layer` and `D2-Layer` show significant performance improvement than all other baselines on `Large`, `Medium`, and `Small` datasets. Also, `D1-Layer` has better performance in defending against adversarial attacks than `D2-Layer` and of cause other baselines.

Let us now demonstrate the effectiveness of our proposed `D-Layers`' robustness by utilizing the robustness definition from Definition 3. In particular, we summarize the number of times a method's robust accuracy wins against the standard accuracy of an `ANN` by a certain margin – denoted as δ, under `LPF`

attack in Table 2 [10]. The results are reported for varying values of δ. It can be seen that `D1-Layer` and `D2-Layer` outperform all other baselines on all values of δ, with `D1-Layer` (as we found earlier) is more robust than `D2-Layer`.

Table 2: Number of Wins of `D1-Layer`, `D2-layer`, `D2A3N`, and `Madry` with varying the value of δ.

δ	`D1-layer` Wins	`D2-layer` Wins	`D2A3N` Wins	`Madry` Wins
δ =**25%**	**17**	**12**	8	10
δ =**30%**	**18**	**13**	11	10
δ =**35%**	**19**	**15**	12	10

4.2.3 Handling covariate drift

The typical way of evaluating the covariate drift handling ability of models is to simulate the drift artificially in the data, then test the models' performance on the drifted data [27]. For doing this, we followed the following procedures:

- We split each dataset into training set and testing set (as described in Section 4.1.4). We will refer to these sets as *training data* and *original test data* respectively, in the following discussions.
- We apply a non-linear transformation to all features ($X_j^i = \alpha {X_j^i}^5 + \beta X_j^i + \gamma$) on the testing set. The values of α, β, and γ are set to 1, 1, 300 for the transformation. We call this dataset as *drifted test data* in the following.
- The `D1-Layer`, `D2-Layer`, `D2A3N`, and `Clean ANN` are trained on the training set and tested on the *drifted test data*.

The average robustness of our proposed `D2-Layer` and baselines under monotonic covariate drift are presented in Figure 7 [11]. We can see that `D2-Layer` achieves the highest average robust accuracy (0.89) and wins against all baselines on `Large`, `Medium`, and `Small` datasets. The average performance improvement of `D2-Layer` compared to `Clean ANN` is 29% (which is quite impressive). This demonstrates the superiority of `D2-Layer` in handling monotonic covariate drift. It can be seen that `D1-Layer` and `D2A3N` can not address monotonic covariate drift at all.

To further demonstrate the effectiveness of `D2-Layer` in handling monotonic covariate drift, we visualize the accuracies of clean `ANN` and `D2-Layer` with and without drift on various datasets in Figure 8. In particular, we plot the accuracies on *modified testing data* and *testing data*. For the sake of completeness, we also plot the model's performance during the training as well. From Figure 8, we can see that during the covariate drift phase, there is a significant performance degradation of clean `ANN` (green line). However, the

[10] Note, we only present results under `LPF` attack as a representative attack and also as it is the most powerful form of attack.

[11] The detailed performance of `D-Layers` and baselines in handling monotonic covariate drift on each dataset are provided in Table 3 of the appendix.

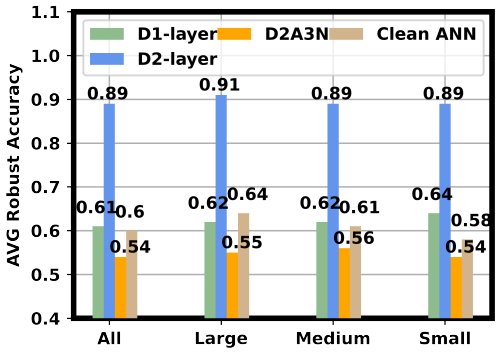

Fig. 7: Robust Accuracy of `D1-Layer`, `D2-Layer`, `D2A3N` and `ANN` under covariate drift.

performance of the `D2-Layer`-based `ANN` model (red line) is maintained, which clearly demonstrates `D2-Layer`'s ability in handling covariate drift. The inclusion of training accuracies in the results reveals that `D2-Layer` has a different convergence profile as compared to clean `ANN`.

4.2.4 Selection of Discretization Strategies in `D2-Layer`

As we discussed in Section 3, `D2-Layer` can accommodate various discretization strategies. So far, in this work, we have constrained `D2-Layer` with equal frequency discretization. In this section, we will study the performance of `D2-Layer` with two other discretization techniques namely – `Equal Width` discretization (denoted as `EW`) and `Quantile`-based discretization technique based on `Keras` discretization layer (denoted as `Quan`). Note, `Equal Frequency` discretization is denoted as `EF` in the results. We have not tested the performance of `D2-Layer` with supervised methods such as `MDL` discretization, because, it is not possible to fix the number of bins with `MDL` discretization. That is, different batches in the data will lead to different numbers of bins. The inclusion of `MDL` discretization in `D2-Layer` has been left as a future work.

The average robust accuracy of `D2-Layer` with the three discretization methods (namely `EF` – default option in `D2-Layer`, `EW`, and `Quan`) under adversarial attacks and covariate drift is shown in Figure 9 [12]. We can see that `D2-Layer` with `EF` discretization (`D2-EF`) achieves better performance than that with `EW` discretization (`D2-EW`) and `quantile`-based discretization (`D2-Quan`).

4.2.5 One Strategy for two Problems

Based on the experimental results in Section 4.2.2 and Section 4.2.3, we can establish that `D2-Layer` is efficient in terms of providing a defence against adversarial attacks as well as handling covariate drift. To clearly demonstrate

[12]The detailed robust accuracy of `D2-Layer` with the three discretization strategies on each dataset is provided in Table 4 of the appendix.

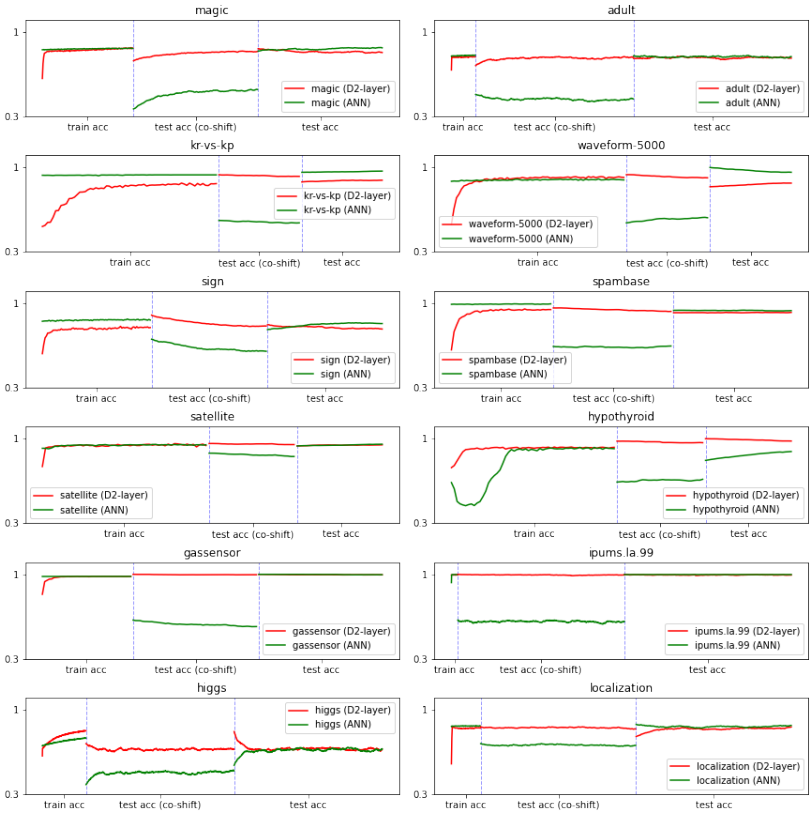

Fig. 8: Illustration of accuracy (with and without covariate drift) on various datasets. Plots show accuracy on the training data (during the training process), followed by accuracy of the trained model on the *drifted testing data*, followed by the accuracy of the trained model on *original testing data*.

this property, we plot the performance of `D2-Layer` under covariate drift and adversarial attack simultaneously, on two datasets, in Figure 10. It can be seen that `D2-Layer`-based `ANN` has a consistent performance under the three attack methods and covariate shift. Its performance is consistently maintained within the $\pm 25\%$ degradation boundaries (shown by orange lines in the figure). In contrast, there is significant performance degradation in the performance of the clean `ANN` model (green line).

5 Conclusions

In this paper, we proposed two `ANN` layers - `D1-Layer` and `D2-Layer` (collectively referred to as `D-Layers`) to improve the robustness of typical `ANN` models on tabular datasets. This is an extension of research focusing on the use of discretization in improving `ANN`'s robustness ([9, 35]). The two layers are motivated by the need of adding discretization within the training of `ANN`

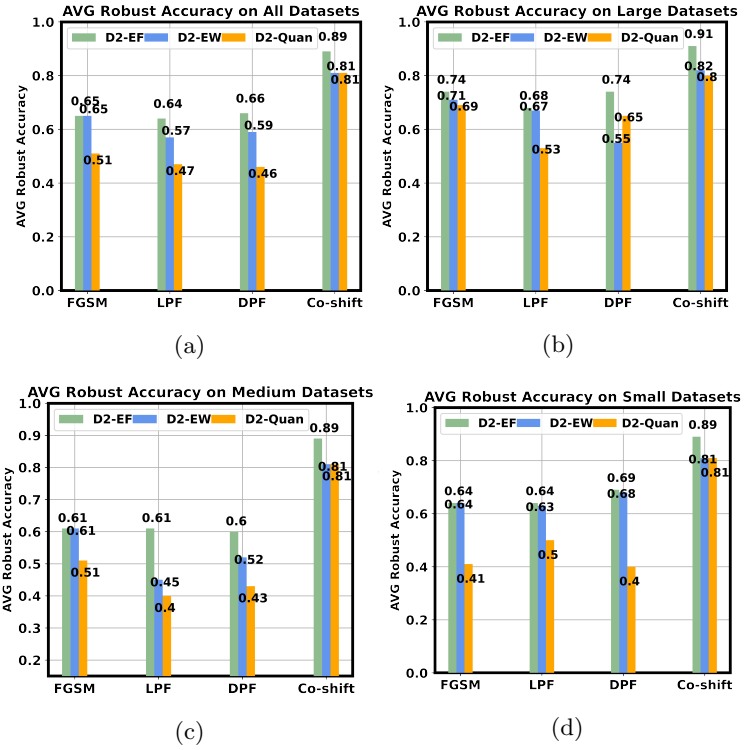

Fig. 9: Robust Accuracy of `D2-Layer` under different discretization strategies (`EF`, `EW` and `Quan`).

models and, therefore, learn cut-point for discretizing the input data during the training phase. Furthermore, `D2-Layer` is motivated by the need for dynamic cut-point adjustment at the testing time. Through empirical evaluations, we demonstrated that `D1-Layer` and `D2-Layer` can be easily integrated into existing `ANN` models and provides an excellent mechanism for defending against adversarial attacks and for addressing some forms of covariate drift. Our experimental results revealed that:

1. `D1-Layer` leads to state-of-the-art (`SOTA`) defence performance against major forms of adversarial attacks on various tabular datasets.
2. `D2-Layer` leads to an effective strategy to address covariate drift and adversarial attacks at the same time.

Our future work entails:

- *Studying the application of `D-Layers` to the hidden layers of the network*: This will result in obtaining a discrete `ANN` and can lead to a network that is more robust to attacks and covariate drift. However, it can result in significant performance degradation. How to maintain a good performance while

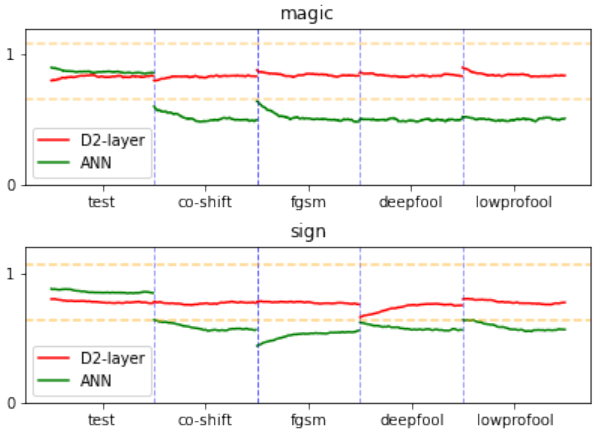

Fig. 10: Illustration of the robustness of `D2-Layer` to adversarial attacks and covariate drift by demonstrating its performance under various forms of attacks as well as covariate drift. Horizontal orange lines depict $\delta = 25\%$. The two models are applied on *testing data*, followed by *drifted testing data*, followed by *modified testing data* (due to `FGSM`, `DPF` and `LPF` attacks).

maintaining robustness is a question of great value, and we are currently investigating this.

- *Studying the impact of the nature of input data*: That is, how the number of features, the number of categorial/numerical features, data size, etc. influence the performance of `D-Layers` in defending against adversarial attacks and addressing co-variate shifts.
- *Studying the efficacy of `D2-Layer` for other forms of drift*: Currently, the proposed `D2-Layer` can only be effective against the monotonic drift in the data. We are currently exploring the effectiveness of `D2-Layer` against non-monotonic transformations as well as concept drifts.

Acknowledgments. The authors would like to thank `Mark James Carman` from Politecnico Di Milano, Italy and `Jiahui Zhou` from the School of Computer Science, Xi'an ShiYou University, for helpful discussions during the course of this research. The first author of the paper is supported by the Australian Government Research Training Program (AGRTP) Scholarship.

A Code

The code of `D-Layers`, as well as the data used in this paper, along with experimental scripts, is available to be used at: https://github.com/allwenau/DLayers.

B Detailed Results

The detailed results of all the experiments done in this paper can be found in Tables 3, 4, 5, 6.

Table 3: Robust Accuracy Comparison of Different Search Strategies for `D1-Layer`.

Datasets	DES			TSES			DCS		
	FGSM	LPF	DPF	FGSM	LPF	DPF	FGSM	LPF	DPF
covtype	0.57	0.58	0.56	0.74	0.65	0.75	0.54	0.52	0.66
census-income	0.97	0.97	0.97	0.96	0.97	0.97	0.95	0.91	0.93
skin-segmentation	0.79	0.79	0.03	0.88	0.81	0.14	0.85	0.84	0.10
localization	0.89	0.89	0.89	0.89	0.89	0.89	0.52	0.39	0.36
accelerometer	0.48	0.48	0.49	0.53	0.48	0.49	0.49	0.53	0.46
higgs	0.54	0.54	0.54	0.51	0.50	0.51	0.53	0.55	0.48
ipums.la.99	0.58	0.58	0.57	0.66	0.92	0.65	0.89	0.95	0.65
connect-4	0.73	0.73	0.73	0.72	0.73	0.70	0.53	0.70	0.82
adult	0.76	0.76	0.76	0.77	0.79	0.79	0.69	0.76	0.66
letter-recog	0.49	0.49	0.49	0.55	0.60	0.50	0.17	0.36	0.33
magic	0.63	0.63	0.63	0.67	0.57	0.75	0.58	0.71	0.78
gassensor	0.52	0.52	0.52	0.72	0.75	0.84	0.78	0.86	0.88
sign	0.57	0.57	0.57	0.39	0.49	0.61	0.38	0.56	0.29
occupancy	0.94	0.94	0.94	0.98	0.95	0.95	1.00	0.89	0.89
satellite	0.57	0.57	0.57	0.84	0.81	0.97	0.67	0.63	0.92
page-blocks	0.91	0.91	0.91	0.92	0.92	0.92	0.91	0.90	0.91
wall-following	0.75	0.75	0.75	0.77	0.70	0.78	0.74	0.70	0.82
spambase	0.48	0.54	0.53	0.56	0.72	0.47	0.44	0.66	0.46
waveform-5000	0.56	0.56	0.56	0.56	0.56	0.56	0.61	0.32	0.60
kr-vs-kp	0.49	0.49	0.49	0.22	0.31	0.15	0.97	0.49	0.90
sick	0.96	0.96	0.96	0.96	0.96	0.96	0.96	0.96	0.96
hypothyroid	0.95	0.95	0.94	0.95	0.95	0.94	0.95	0.95	0.94
cmc	0.63	0.63	0.63	0.63	0.63	0.61	0.63	0.63	0.63
german	0.68	0.68	0.68	0.56	0.62	0.44	0.68	0.69	0.63
Average (All)	0.68	0.69	0.65	**0.71**	**0.72**	**0.68**	0.69	0.69	0.67
Average (Large)	0.74	0.74	0.59	**0.80**	**0.76**	**0.65**	0.67	0.64	0.50
Average (Medium)	0.64	0.64	0.64	**0.66**	**0.70**	**0.70**	0.62	0.71	0.64
Average (Small)	0.70	0.70	0.70	**0.70**	**0.72**	**0.68**	0.76	0.69	0.78

References

[1] Goodfellow, I.J., Shlens, J., Szegedy, C.: Explaining and harnessing adversarial examples. arXiv preprint arXiv:1412.6572 (2014)

[2] Kurakin, A., Goodfellow, I.J., Bengio, S.: Adversarial machine learning at scale. In: 5th International Conference on Learning Representations, ICLR 2017 - Conference Track Proceedings (2017). Cited By :374

Table 4: Robust Accuracy of `D1-layer`, `D2-layer` and Baselines Under Adversarial Attacks. The last column of the table presents `ANN`'s accuracy without attacks on each dataset, i.e., standard accuracy of each dataset.

Datasets	D1-layer			D2-layer			D2A3N			Madry			Clean ANN			ANN
	FGSM	LPF	DPF	FGSM	LPF	DPF	FGSM	LPF	DPF	FGSM	LPF	DPF	FGSM	LPF	DPF	Std Acc
covtype	0.74	0.65	0.75	0.46	0.40	0.58	0.57	0.64	0.57	0.58	0.58	0.42	0.35	0.37	0.07	0.93
census-income	0.96	0.97	0.95	0.95	0.87	0.97	0.96	0.97	0.96	0.96	0.96	0.96	0.48	0.20	0.05	0.97
skin-segmentation	0.88	0.81	0.14	0.90	0.81	0.79	0.83	0.90	0.09	0.83	0.80	0.04	0.78	0.78	0.28	0.99
localization	0.89	0.89	0.89	0.87	0.78	0.84	0.58	0.41	0.52	0.64	0.42	0.50	0.45	0.49	0.42	0.86
accelerometer	0.53	0.48	0.49	0.51	0.53	0.50	0.54	0.52	0.55	0.54	0.46	0.48	0.51	0.46	0.35	0.64
higgs	0.51	0.50	0.51	0.44	0.58	0.49	0.48	0.47	0.43	0.53	0.51	0.54	0.39	0.34	0.36	0.68
ipums.la.99	0.66	0.92	0.65	0.98	0.97	0.58	0.57	0.78	0.57	0.92	0.92	0.54	0.68	0.12	0.02	1.00
connect-4	0.72	0.73	0.70	0.52	0.52	0.54	0.27	0.46	0.33	0.38	0.47	0.61	0.18	0.15	0.31	0.83
adult	0.77	0.79	0.79	0.66	0.59	0.59	0.48	0.39	0.33	0.69	0.64	0.66	0.29	0.34	0.35	0.80
letter-recog	0.55	0.60	0.50	0.51	0.07	0.53	0.17	0.01	0.22	0.16	0.01	0.38	0.12	0.01	0.03	0.99
magic	0.67	0.57	0.75	0.49	0.57	0.57	0.27	0.21	0.36	0.39	0.19	0.61	0.19	0.12	0.15	0.85
gassensor	0.72	0.75	0.84	0.62	0.42	0.78	0.59	0.48	0.66	0.33	0.05	0.34	0.32	0.00	0.01	0.99
sign	0.39	0.49	0.61	0.31	0.81	0.45	0.25	0.32	0.28	0.25	0.25	0.25	0.23	0.23	0.21	0.82
occupancy	0.98	0.95	0.95	0.92	0.94	0.83	0.99	0.90	0.98	1.00	1.00	0.98	0.69	0.13	0.32	1.00
satellite	0.84	0.81	0.97	0.75	0.81	0.94	0.75	0.26	0.93	0.73	0.39	0.97	0.45	0.08	0.24	0.98
page-blocks	0.92	0.92	0.92	0.62	0.74	0.61	0.13	0.68	0.27	0.04	0.02	0.37	0.04	0.02	0.40	0.98
wall-following	0.77	0.70	0.78	0.60	0.54	0.75	0.48	0.61	0.64	0.35	0.50	0.45	0.25	0.16	0.19	0.98
waveform-5000	0.56	0.72	0.47	0.54	0.55	0.44	0.34	0.51	0.32	0.29	0.06	0.21	0.22	0.06	0.07	0.91
spambase	0.56	0.56	0.56	0.24	0.18	0.56	0.10	0.48	0.10	0.10	0.17	0.12	0.09	0.09	0.56	0.94
kr-vs-kp	0.22	0.31	0.15	0.51	0.47	0.51	0.23	0.25	0.20	0.74	0.40	0.47	0.42	0.03	0.04	0.95
sick	0.96	0.96	0.96	0.94	0.96	0.96	0.88	0.90	0.77	0.45	0.54	0.30	0.42	0.38	0.45	0.92
hypothyroid	0.95	0.95	0.94	0.93	0.90	0.92	0.95	0.84	0.94	0.95	0.95	0.94	0.36	0.55	0.57	0.98
cmc	0.63	0.63	0.61	0.53	0.59	0.53	0.65	0.67	0.68	0.64	0.60	0.61	0.47	0.39	0.36	0.70
german	0.56	0.62	0.44	0.69	0.68	0.69	0.61	0.64	0.53	0.69	0.67	0.41	0.50	0.29	0.31	0.71
Average (All)	**0.71**	**0.72**	**0.68**	**0.65**	**0.64**	**0.66**	0.53	0.55	0.51	0.55	0.48	0.51	0.37	0.24	0.26	0.89
Average (Large)	**0.80**	**0.76**	**0.65**	**0.74**	**0.68**	**0.74**	0.70	0.69	0.54	0.71	0.64	0.48	0.51	0.46	0.23	0.88
Average (Medium)	**0.66**	**0.70**	**0.70**	**0.61**	**0.61**	**0.60**	0.45	0.45	0.46	0.70	0.63	0.50	0.34	0.16	0.20	0.88
Average (Small)	**0.70**	**0.72**	**0.68**	**0.64**	**0.64**	**0.69**	0.51	0.58	0.54	0.50	0.43	0.48	0.32	0.21	0.32	0.91

[3] Akhtar, N., Mian, A.: Threat of adversarial attacks on deep learning in computer vision: A survey. Ieee Access **6**, 14410–14430 (2018)

[4] Shafahi, A., Najibi, M., Ghiasi, A., Xu, Z., Dickerson, J., Studer, C., Davis, L.S., Taylor, G., Goldstein, T.: Adversarial training for free! In: Advances in Neural Information Processing Systems, vol. 32 (2019). Cited By :92

[5] Cartella, F., Anunciação, O., Funabiki, Y., Yamaguchi, D., Akishita, T., Elshocht, O.: Adversarial attacks for tabular data: application to fraud detection and imbalanced data. In: CEUR Workshop Proceedings, vol. 2808 (2021)

[6] Buckman, J., Roy, A., Raffel, C., Goodfellow, I.: Thermometer encoding: One hot way to resist adversarial examples. In: International Conference on Learning Representations (2018)

[7] Nado, Z., Padhy, S., Sculley, D., D'Amour, A., Lakshminarayanan, B., Snoek, J.: Evaluating prediction-time batch normalization for robustness under covariate shift. arXiv preprint arXiv:2006.10963 (2020)

[8] Magliacane, S., van Ommen, T., Claassen, T., Bongers, S., Versteeg, P., Mooij, J.M.: Domain adaptation by using causal inference to predict invariant conditional distributions. arXiv preprint arXiv:1707.06422 (2017)

Table 5: Robust Accuracy of `D1-Layer`, `D2-Layer`, `D2A3N` and Clean `ANN` Under covariate drift.

Datasets	D1-Layer	D2-Layer	D2A3N	Clean ANN
covtype	0.43	0.87	0.43	0.57
census-income	0.29	0.90	0.94	0.38
skin-segmentation	0.79	0.97	0.94	0.79
localization	0.81	0.96	0.50	0.81
accelerometer	0.31	0.86	0.21	0.39
higgs	0.72	0.89	0.92	0.72
ipums.la.99	0.70	0.91	0.47	0.70
connect-4	0.70	0.89	0.58	0.65
adult	0.66	0.89	0.73	0.61
letter-recog	0.66	0.89	0.24	0.61
magic	0.65	0.89	0.47	0.60
gassensor	0.65	0.89	0.65	0.60
sign	0.65	0.89	0.47	0.60
occupancy	0.29	0.90	0.50	0.38
satellite	0.65	0.89	0.48	0.60
page-blocks	0.65	0.89	0.93	0.60
wall-following	0.65	0.89	0.72	0.60
spambase	0.65	0.89	0.51	0.60
waveform-5000	0.65	0.89	0.59	0.60
kr-vs-kp	0.65	0.89	0.51	0.60
sick	0.65	0.89	0.06	0.60
hypothyroid	0.65	0.89	0.05	0.61
cmc	0.65	0.89	0.64	0.61
german	0.65	0.89	0.70	0.61
Average (ALL)	0.61	**0.89**	0.54	0.60
Average (Large)	0.62	**0.91**	0.55	0.64
Average (Medium)	0.62	**0.89**	0.56	0.61
Average (Small)	0.64	**0.89**	0.54	0.58

[9] Zhou, J., Zaidi, N., Zhang, Y., Li, G.: Discretization inspired defence algorithm against adversarial attacks on tabular data. In: Pacific-Asia Conference on Knowledge Discovery and Data Mining, pp. 367–379 (2022). Springer

[10] Kumová, V., Pilát, M.: Beating white-box defenses with black-box attacks. In: 2021 International Joint Conference on Neural Networks (IJCNN), pp. 1–8 (2021). IEEE

[11] Huang, X., Kroening, D., Ruan, W., Sharp, J., Sun, Y., Thamo, E., Wu, M., Yi, X.: A survey of safety and trustworthiness of deep neural networks: Verification, testing, adversarial attack and defence, and interpretability. Computer Science Review **37**, 100270 (2020)

[12] Kong, Z., Xue, J., Wang, Y., Huang, L., Niu, Z., Li, F.: A survey on adversarial attack in the age of artificial intelligence. Wireless Communications and Mobile Computing **2021** (2021)

[13] Kurakin, A., Goodfellow, I., Bengio, S.: Adversarial machine learning at

Table 6: Robust Accuracy of `D2-layer` with Different Discretiztaion Strategy Under Adversarial Attacks or Covariate Shift.

Datasets	D2-EF				D2-EW				D2-Quan			
	FGSM	LPF	DPF	Co-shift	FGSM	LPF	DPF	Co-shift	FGSM	LPF	DPF	Co-shift
covtype	0.46	0.40	0.58	0.87	0.37	0.44	0.58	0.75	0.55	0.48	0.55	0.72
census-income	0.95	0.87	0.97	0.90	0.87	0.74	0.03	0.82	0.93	0.46	0.87	0.80
skin-segmentation	0.90	0.81	0.79	0.97	0.89	0.82	0.79	0.84	0.83	0.80	0.79	0.84
localization	0.87	0.78	0.84	0.94	0.88	0.82	0.89	0.85	0.64	0.40	0.53	0.84
accelerometer	0.51	0.53	0.50	0.86	0.55	0.51	0.48	0.82	0.50	0.49	0.49	0.82
higgs	0.44	0.58	0.49	0.89	0.47	0.52	0.49	0.80	0.43	0.47	0.44	0.80
ipums.la.99	0.98	0.97	0.58	0.91	0.95	0.93	0.42	0.81	0.90	0.95	0.58	0.81
connect-4	0.52	0.52	0.54	0.89	0.76	0.63	0.74	0.81	0.53	0.48	0.50	0.81
adult	0.66	0.59	0.59	0.89	0.76	0.56	0.62	0.81	0.73	0.45	0.45	0.81
letter-recog	0.51	0.07	0.53	0.89	0.39	0.05	0.48	0.81	0.13	0.01	0.25	0.81
magic	0.49	0.57	0.57	0.89	0.49	0.41	0.59	0.81	0.32	0.33	0.48	0.81
gassensor	0.62	0.42	0.78	0.89	0.30	0.46	0.52	0.81	0.41	0.38	0.63	0.81
sign	0.31	0.81	0.45	0.89	0.41	0.40	0.51	0.81	0.28	0.33	0.49	0.81
occupancy	0.92	0.94	0.83	0.90	0.99	0.05	0.28	0.81	0.88	0.16	0.04	0.81
satellite	0.75	0.81	0.94	0.89	0.69	0.59	0.95	0.81	0.53	0.58	0.94	0.81
page-blocks	0.62	0.74	0.61	0.89	0.41	0.84	0.55	0.81	0.12	0.19	0.07	0.81
wall-following	0.60	0.54	0.75	0.89	0.75	0.72	0.75	0.81	0.53	0.66	0.66	0.81
waveform-5000	0.54	0.55	0.44	0.89	0.42	0.31	0.48	0.81	0.34	0.25	0.36	0.81
spambase	0.24	0.18	0.56	0.89	0.10	0.20	0.56	0.81	0.10	0.15	0.08	0.81
kr-vs-kp	0.51	0.47	0.51	0.89	0.95	0.62	0.67	0.81	0.11	0.18	0.02	0.81
sick	0.94	0.96	0.96	0.89	0.93	0.93	0.78	0.81	0.70	0.85	0.62	0.81
hypothyroid	0.93	0.90	0.92	0.89	0.87	0.76	0.95	0.81	0.42	0.92	0.21	0.81
cmc	0.53	0.59	0.53	0.89	0.64	0.56	0.58	0.81	0.62	0.54	0.58	0.81
german	0.69	0.68	0.69	0.89	0.68	0.72	0.56	0.81	0.63	0.66	0.46	0.81
Average (All)	**0.65**	**0.64**	**0.66**	**0.89**	0.65	0.57	0.59	0.81	0.51	0.47	0.46	0.81
Average (Large)	0.74	0.68	0.74	0.91	0.71	0.67	0.55	0.82	0.69	0.53	0.65	0.80
Average (Medium)	0.61	0.61	0.60	0.89	0.61	0.45	0.52	0.81	0.51	0.40	0.43	0.81
Average (Small)	0.64	0.64	0.69	0.89	0.64	0.63	0.68	0.81	0.41	0.50	0.40	0.81

scale. arXiv preprint arXiv:1611.01236 (2016)

[14] Madry, A., Makelov, A., Schmidt, L., Tsipras, D., Vladu, A.: Towards deep learning models resistant to adversarial attacks. arXiv preprint arXiv:1706.06083 (2017)

[15] Moosavi-Dezfooli, S.-M., Fawzi, A., Frossard, P.: Deepfool: a simple and accurate method to fool deep neural networks. In: Proceedings of the IEEE Conference on Computer Vision and Pattern Recognition, pp. 2574–2582 (2016)

[16] Ballet, V., Renard, X., Aigrain, J., Laugel, T., Frossard, P., Detyniecki, M.: Imperceptible adversarial attacks on tabular data. arXiv preprint arXiv:1911.03274 (2019)

[17] Sugiyama, M., Krauledat, M., Müller, K.-R.: Covariate shift adaptation by importance weighted cross validation. Journal of Machine Learning Research **8**(5) (2007)

[18] Bickel, S., Brückner, M., Scheffer, T.: Discriminative learning under covariate shift. Journal of Machine Learning Research **10**(9) (2009)

[19] Gama, J., Žliobaitė, I., Bifet, A., Pechenizkiy, M., Bouchachia, A.: A

survey on concept drift adaptation. ACM computing surveys (CSUR) **46**(4), 1–37 (2014)

[20] Chen, M., Zhao, S., Liu, H., Cai, D.: Adversarial-learned loss for domain adaptation. In: Proceedings of the AAAI Conference on Artificial Intelligence, vol. 34, pp. 3521–3528 (2020)

[21] Wang, B., Qiu, M., Wang, X., Li, Y., Gong, Y., Zeng, X., Huang, J., Zheng, B., Cai, D., Zhou, J.: A minimax game for instance based selective transfer learning. In: Proceedings of the 25th ACM SIGKDD (2019)

[22] Wilson, G., Cook, D.J.: A survey of unsupervised deep domain adaptation. ACM Transactions on Intelligent Systems and Technology (TIST) (2020)

[23] Gretton, A., Smola, A., Huang, J., Schmittfull, M., Borgwardt, K., Schölkopf, B.: Covariate shift by kernel mean matching. Dataset shift in machine learning **3**(4), 5 (2009)

[24] Li, F., Lam, H., Prusty, S.: Robust importance weighting for covariate shift. In: International Conference on Artificial Intelligence and Statistics, pp. 352–362 (2020). PMLR

[25] Zhang, T., Yamane, I., Lu, N., Sugiyama, M.: A one-step approach to covariate shift adaptation. In: Asian Conference on Machine Learning, pp. 65–80 (2020). PMLR

[26] Pathak, R., Ma, C., Wainwright, M.: A new similarity measure for covariate shift with applications to nonparametric regression. In: International Conference on Machine Learning, pp. 17517–17530 (2022). PMLR

[27] Nair, N.G., Satpathy, P., Christopher, J., *et al.*: Covariate shift: A review and analysis on classifiers. In: 2019 Global Conference for Advancement in Technology (GCAT), pp. 1–6 (2019). IEEE

[28] Yu, Z., Wang, P., Xu, J., Xie, L., Jin, Z., Huang, J., He, X., Cai, D., Hua, X.-S.: Stable learning via causality-based feature rectification. CoRR (2020)

[29] Pfahringer, B., Holmes, G., Kirkby, R.: New options for Hoeffding trees. In: AI 2007: Advances in Artificial Intelligence vol. 4830, pp. 90–99 (2007). Springer

[30] Bifet, A., Gavaldà, R.: Adaptive learning from evolving data streams. In: Advances in Intelligent Data Analysis VIII, pp. 249–260 (2009). Springer

[31] Oza, N., Russell, S.: Online bagging and boosting. In: Artificial Intelligence and Statistics 2001, pp. 105–112 (2001). Morgan Kaufmann

[32] Ioffe, S., Szegedy, C.: Batch normalization: Accelerating deep network training by reducing internal covariate shift. In: International Conference on Machine Learning (2015). PMLR

[33] Van Den Oord, A., Vinyals, O., et al.: Neural discrete representation learning. Advances in neural information processing systems **30** (2017)

[34] Bengio, Y., Léonard, N., Courville, A.: Estimating or propagating gradients through stochastic neurons for conditional computation. arXiv preprint arXiv:1308.3432 (2013)

[35] Zhou, J., Zaidi, N., Zhang, Y., Montague, P., Kim, J., Li, G.: Leveraging generative models for combating adversarial attacks on tabular datasets. In: Pacific-Asia Conference on Knowledge Discovery and Data Mining, pp. 147–158 (2023). Springer